

# Apple Polyphenol Phloretin Potentiates the Anticancer Actions of Paclitaxel Through Induction of Apoptosis in Human Hep G2 Cells

Kuo-Ching Yang,<sup>1</sup> Chia-Yi Tsai,<sup>2</sup> Ying-Jan Wang,<sup>3</sup> Po-Li Wei,<sup>4</sup> Chia-Hwa Lee,<sup>5</sup> Jui-Hao Chen,<sup>1</sup> Chih-Hsiung Wu,<sup>6\*\*</sup> and Yuan-Soon Ho<sup>5\*</sup>

<sup>1</sup>Division of Gastroenterology, Department of Internal Medicine, Shin Kong Wu Ho-Su Memorial Hospital, School of Medicine, Taipei Medical University, Taipei, Taiwan

<sup>2</sup>Division of Transfusion Medicine, Department of Pathology and Laboratory Medicine, Shin Kong Wu Ho-Su Memorial Hospital Taipei, Taiwan

<sup>3</sup>Department of Environmental and Occupational Health, National Cheng Kung University Medical College, Tainan, Taiwan

<sup>4</sup>Department of Surgery, Graduate Institute of Clinical Medicine, Taipei Medical University Hospital, Taipei Medical University, Taipei, Taiwan

<sup>5</sup>Graduate Institute of Biomedical Technology, Taipei Medical University, Taipei, Taiwan

<sup>6</sup>Department of Surgery, School of Medicine, Taipei Medical University and Hospital, Taipei, Taiwan

Phloretin (Ph), which can be obtained from apples, apple juice, and cider, is a known inhibitor of the type II glucose transporter (GLUT2). In this study, real-time PCR analysis of laser-capture microdissected (LCM) human hepatoma cells showed elevated expression (>5-fold) of GLUT2 mRNA in comparison with nonmalignant hepatocytes. In vitro and in vivo studies were performed to assess Ph antitumor activity when combined with paclitaxel (PTX) for treatment of human liver cancer cells. Inhibition of GLUT2 by Ph potentiated the anticancer effects of PTX, resensitizing human liver cancer cells to drugs. These results demonstrate that 50–150  $\mu$ M Ph significantly potentiates DNA laddering induced in Hep G2 cells by 10 nM PTX. Activity assays showed that caspases 3, 8, and 9 are involved in this apoptosis. The antitumor therapeutic efficacy of Ph (10 mg/kg body weight) was determined in cells of the SCID mouse model that were treated in parallel with PTX (1 mg/kg body weight). The Hep G2-xenografted tumor volume was reduced more than fivefold in the Ph + PTX-treated mice compared to the PTX-treated group. These results suggest that Ph may be useful for cancer chemotherapy and chemoprevention. © 2008 Wiley-Liss, Inc.

**Key words:** apoptosis; glucose transporters; Hep G2 cells; phloretin; paclitaxel

## INTRODUCTION

Glucose transport across the plasma membrane is the rate-limiting step in its subsequent utilization, and it is mediated by specific glucose transporter (GLUT) proteins. There are 14 members in the mammalian glucose transporter (GLUT) family, including GLUT1 through GLUT12, GLUT14, and the Ht/myo-inositol transporters [1]. Among normal human tissues, GLUT2 is present in the liver, pancreatic B-cells, hypothalamic glial cells, the retina, and erythrocytes [2,3]. Increased expression of GLUT2 has been found in many human tumor tissues, including hepatic, breast, and gastric cancer cells [1,4–6]. Previous studies have demonstrated the absence of GLUT1 expression in human hepatoma cells [7,8]. In this study, levels of GLUT2 mRNA expression were found to be more than fivefold higher in human liver tumor tissues than in normal liver tissue. Such observations prompted us to test whether GLUT2 expression is important for human liver cancer cell survival and to assess whether the

inhibition of glucose uptake could serve as an efficient strategy for cancer therapy.

Phloretin (Ph), a natural polyphenolic compound found in apples and pears, has been shown to exert anti-tumor activity through its inhibition of protein kinase C (PKC) activity and its induction of apoptosis [9]. On the other hand, it has also been suggested that Ph is a specific GLUT2 inhibitor [10,11]. A recent

Abbreviations: glucose transporter (GLUT); phloretin or 2',4',6'-trihydroxy-3-(*p*-hydroxyphenyl)propiophenone (Ph); protein kinase C (PKC); paclitaxel (PTX); *p*-nitroaniline (*p*NA);  $\beta$ -glucuronidase (GUS); laser capture microdissection (LCM).

\*Correspondence to: Graduate Institute of Biomedical Technology, Taipei Medical University, 250 Wu-Hsing Street, Taipei 110, Taiwan.

\*\*Correspondence to: Department of Surgery, School of Medicine, Taipei Medical University and Hospital, No. 252 Wu-Hsing Street, Taipei 110, Taiwan.

Received 5 June 2008; Revised 26 July 2008; Accepted 5 August 2008

DOI 10.1002/mc.20480

Published online 2 September 2008 in Wiley InterScience (www.interscience.wiley.com)

study demonstrated that Ph ( $IC_{50} = 0.8 \mu\text{M}$ ) isolated from the Formosan apple (*Malus doumeri* var. *formosana*), an indigenous Taiwanese plant, is the most potent component of the anti-tumor extract. This Ph exhibited significant hydroxyl radical-scavenging activity in cultured primary human melanocytes [12]. Ph at concentrations of 50–500  $\mu\text{M}$  has been shown not only to block eukaryotic urea transporters [13,14] but also to efficiently inhibit the toxic effects of the cytotoxin VacA ( $IC_{50} = 15 \mu\text{M}$ ), which is the major virulence factor of the human pathogen *Helicobacter pylori* [14]. Another study demonstrated that Ph at 30  $\mu\text{M}$  acts as a lipophilic dipolar substance that decreases the membrane dipole potential, leading not only to reduced accumulation of  $\beta$ -amyloid peptides ( $A\beta$ ) into senile plaques, but also to reduced  $A\beta$  toxicity in neuron-like PC12 cells. In contrast, Ph at 300  $\mu\text{M}$  was toxic to these cells [15].

The microtubule-stabilizing paclitaxel (PTX) has a taxane structure (MW 853.9), and it can be half-synthesized using 10-deacetylbaccatine extracted from the Pacific yew tree (*Taxus brevifolia*) [16]. The albumin-bound form of PTX (Abraxane®) is a clinical product that is used in a formulation with a mean particle size of approximately 130 nm. It has a high affinity for microtubules and it enhances tubulin polymerization, causing mitosis (M) phase cell cycle arrest [17]. Side-effects induced by PTX include myelosuppression, neurotoxicity, asthenia, fatigue, and weakness [18]. Impaired liver function has also been observed in patients administered PTX as an anticancer agent [19]. Although the recommended dosage of PTX is 210 mg/m<sup>2</sup>, side effects such as leukocyte reduction and neutropenia can already be observed at this dosage. There is an urgent need to develop more effective therapeutic strategies involving PTX that cause fewer side effects.

The present study took advantage of the previously reported ability of PTX to trigger apoptosis in human Hep G2 and Hep 3B cells [20]. Treatment plans that combine the use of PTX with antineoplastic drugs such as 5-fluorouracil (5-FU) or cisplatin significantly enhance the apoptotic effect of PTX in human hepatoma cell lines [20]. The present study sought to extend these results by evaluating the cytotoxic effects of Ph and PTX, which have different cellular targets, in a variety of human cancers—COLO 205, HT 29, Hep G2, Hep 3B, and HL 60—and normal human colon epithelial (FHC) cell lines. The cancer cells used in this study were chosen to have different p53 status [21], because it is important to investigate whether regulators other than p53 participate in Ph-mediated cytotoxicity. The results from this study provide clear evidence that Ph significantly potentiates PTX-induced apoptosis in human hepatoma cells. These results support the use of Ph in cancer chemoprevention and possibly also in chemotherapy.

## MATERIALS AND METHODS

### Chemicals and Reagents

Phloretin (2',4',6'-trihydroxy-3-(*p*-hydroxyphenyl)propiophenone) (purity >99%) and protease inhibitors (phenylmethyl sulfonyl fluoride (PMSF), pepstatin A, leupeptin, and aprotinin) were purchased from Sigma Chemical Company (Sigma Aldrich Chemicals, GmbH, Steinheim, Germany). Dulbecco's modified Eagle's medium (DMEM), fetal calf serum (FCS), penicillin/streptomycin solution, and fungizone were purchased from Gibco-Life Technologies (Paisley, UK).

### Antibodies

The following monoclonal antibodies were obtained from various sources as indicated: anti-caspase-8, anti-cytochrome *c*, anti-Bax, anti-Apaf-1, anti-Bcl-2, anti-Aif, anti-p53, anti-Bid, and anti-GAPDH antibodies (Santa Cruz Biotechnology, Santa Cruz, CA); anti-caspase 9 and anti-caspase 3 antibodies (Stressgen Biotechnologies, Victoria, British Columbia, Canada); anti-PCNA antibody (Dako Corporation, Glostrup, Denmark); and anti-cytochrome *c* oxidase antibody (Research Diagnostics, Flanders, NJ).

### Cell Lines, Cell Culture, and Determination of Cell Growth Curve

The HT 29 (p53 mutant) [22] and COLO 205 (p53 wild) [23] cell lines were isolated from human colon adenocarcinoma (American Type Culture Collection (ATCC) HTB-38 and CCL-222). Hep 3B (p53 partially deleted) [24] and Hep G2 (p53 wild) [24] cell lines were derived from human hepatocellular carcinoma (ATCC HB-8064 and HB-8065). The FHC cell line (CRL-1831; American Type Culture Collection) was a primary cell line derived from long-term epithelial cell cultures of human fetal normal colonic mucosa [25]. The HL 60 cell line (p53 null) was derived from human myeloid leukemia cells (59170; American Type Culture Collection). Cell lines were cultured in essential medium and appropriate conditions as described in our previous papers [26,27]. A total of  $1 \times 10^4$  cells were plated in a 35-mm Petri dish and treated with Ph for cell growth proliferation assays.

### Protein Extraction, Immunoprecipitation, and Western Blot Analysis

Hep G2 cells treated with DMSO, Ph, PTX, or Ph and PTX were harvested for protein extraction as we described previously [27]. To confirm equal loading of proteins, the blots were immunoprobed with a rabbit polyclonal antibody against GAPDH. Equal amounts of protein were immunoprecipitated with saturating amounts of anti-cytochrome *c* antibody. The cytochrome *c*-immunoprecipitated Apaf-1 protein was then evaluated by Western blot.

### Isolation of Mitochondria and Cytosolic Fractions of Cell Lysates

The Hep G2 cells were exposed to Ph (50–100  $\mu$ M), PTX (10 nM), or combined treatment with both compounds for 24 h and then assayed for the translocation of cytochrome *c* from the mitochondrial membrane to the cytosol or the reverse translocation of Bax. Lysis of cells for mitochondrial protein extraction were fractionated according to our previously published method [27]. Blots were probed with a mouse monoclonal antiserum specific for cytochrome *c* (Santa Cruz Biotechnology) or with a rabbit polyclonal antibody specific for cytochrome *c* oxidase, followed by the appropriate secondary antibodies conjugated to horseradish peroxidase (Santa Cruz Biotechnology) for used as a control to demonstrate that mitochondrial protein was successfully fractionated.

### Preparation of Nuclear and Cytoplasmic Fractions

Nuclear and cytoplasmic fractions from control (DMSO-treated) and drug-treated Hep G2 cells were prepared as described previously [28]. The nuclear extract was prepared using the same lysis buffer and stored at  $-80^{\circ}\text{C}$  until use for Western blot analysis of Aif. The blot was stripped and reprobed with anti-PCNA antibody to ensure equal protein loading, as well as to rule out cross contamination of cytoplasmic and nuclear fractions.

### Caspase Activity Assays

Caspase activity was measured using caspases 3, 8 (Promega, Madison, WI), and 9 (Chemicon, Temecula, CA) colorimetric activity assay kits as previously described [29,30]. Caspase activity was measured by the release of *p*-nitroaniline (*p*NA) from the labeled substrates, Ac-DEVD-*p*NA, Ac-IETD-*p*NA, and Ac-LEHD-*p*NA for caspases 3, 8, and 9, respectively, and the free *p*NA was quantified at 405 nm.

### Flow Cytometry and DNA Fragmentation Analysis

The cell cycle stages in the Ph-, PTX-, combination- or DMSO-treated groups were determined by flow cytometry analysis [21]. After treatment, the DNA fragmentation analysis was performed as previously described [21].

### Immunocytochemical Staining Analysis

Human liver cancer tissues from paraffin-embedded blocks were sectioned at 5–7  $\mu$ m thickness, deparaffinized, and rehydrated in PBS according to our previous papers described [21,27]. The primary antibody used in this study was raised against the C-terminal oligopeptide predicted from the rat GLUT2 DNA sequence. The specificity of this antibody was reported previously [1,31,32]. Negative controls were performed using antibody that was preabsorbed with human synthetic GLUT2 peptides

(Santa Cruz Biotechnology) to determine the specificity of the primary antibody.

### Real-Time PCR Analysis

A LightCycler thermocycler was used to conduct real-time PCR (Roche Molecular Biochemicals, Mannheim, Germany). The following concentrations proved optimal: forward primer, 0.5  $\mu$ M; reverse primer, 0.5  $\mu$ M; Taqman probe, 0.1 M; and  $\text{MgCl}_2$ , 5.0 mM. PCR-grade sterile  $\text{H}_2\text{O}$  was used to adjust the final reaction volume as per the manufacturer's instructions. Each genomic equivalent of positive-control DNA was added in a 2  $\mu$ L volume to 18  $\mu$ L of master mix. No-template controls were prepared by adding 2  $\mu$ L of PCR-grade sterile  $\text{H}_2\text{O}$  to 18  $\mu$ L of master mix. Primers used for amplification were as follows: GLUT2 specific primer, GLUT2-f (5'-AGTT-AGATGAGGAAGTCAAAGCAA-3') and GLUT2-r (5'-TAGGCTGTCGGTAGCTGG-3'). The  $\beta$ -glucuronidase (GUS) specific PCR products from the same RNA samples were amplified and served as internal controls. Primers GUS-f (5'-AAACAGCCCCGTTTACTTGAG-3') and GUS-r (5'-AGTGTTCCTGCTAGAA-TAGATG-3') were used for amplification of GUS. A cycle of melting curve analysis for the PCR products was then performed to confirm PCR accuracy with the primers. A previous study found that GUS and 18S rRNA were better housekeeping genes than GAPDH to control for the expression of tumor antigens using real-time PCR [33]. Therefore, in this study, the GLUT2 mRNA fluorescence intensity was normalized with GUS using the Roche LightCycler Software.

### Laser Capture Microdissection (LCM)

The sections stained with hematoxylin/eosin were subjected to LCM by using a PixCell Iie system (Arcturus Engineering, Mountain View, CA) [34]. The parameters used for LCM included a laser diameter of 7.5  $\mu$ m and laser power of 48–65 mW. Per specimen, 15 000 laser pulse discharges were used to capture  $\sim 10$  000 morphologically normal epithelial cells or malignant cell carcinoma cells for each case. Each population was visualized under a microscope to make sure that the captured cells were homogeneous. The caps with the captured cells were then fitted onto 0.5-mL Eppendorf tubes containing 42  $\mu$ L DNA lysis buffer.

### Treatment of Hep G2-Derived Xenografts In Vivo

Hep G2 cells ( $5 \times 10^6$ ) in 0.2 mL were injected subcutaneously between the scapulae of each NOD.CB17-PRKDC(SCID)/J (NOD-SCID) mouse (purchased from the Animal Center of National Cheng Kung University, Tainan, Taiwan). Mice at 6–7 wk of age were used in the experiments as described previously [17,21]. After transplantation, tumor size was measured using calipers, and the tumor volume



was estimated according to the following formula: tumor volume ( $\text{mm}^3$ ) =  $L \times W^2/2$ , where  $L$  and  $W$  are the length and width of the tumor, respectively [17]. Once tumors reached a mean size of  $200 \text{ mm}^3$ , animals received intraperitoneal injections of either Ph (10 mg/kg), PTX (1 mg/kg), both agents, or  $25 \mu\text{L}$  DMSO plus  $25 \mu\text{L}$  peanut oil thrice weekly for 6 wk.

**Statistics**

All of the experimental data are expressed as mean  $\pm$  SEM. Differences in tumor volumes were determined by Student's *t*-test using the Minitab (version 10.2) software package. We assigned statistical significance if  $P < 0.05$ .

**RESULTS**

**Detection of Higher GLUT2 Expression Levels in Human Liver Cancer Cells**

The expression of glucose transporters (GLUTs) in rat hepatocytes has been studied using isoform-specific antibodies. This strategy has demonstrated that the type II glucose transporter (GLUT2) is present in hepatocytes [35,36]. In the present study, cancerous and normal human liver cells were harvested by LCM (Figure 1A), and their GLUT2 mRNA levels were determined using real-time PCR analysis (Figure 1B). Our results showed that GLUT2 mRNA was present at a level more than fivefold higher in human hepatoma cells than in normal

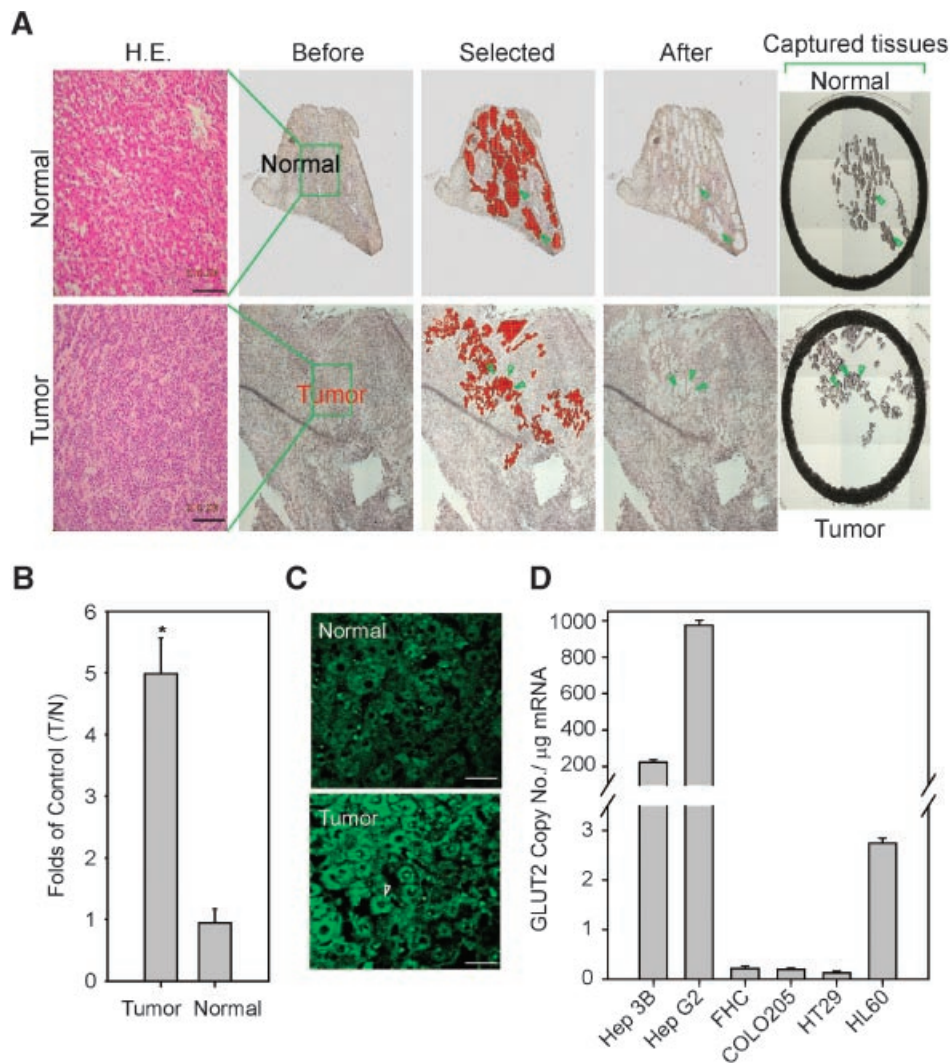


Figure 1. Determination of GLUT2 expression levels in LCM-isolated human hepatocellular carcinoma and normal liver cells. (A) Human liver cells were dissected from liver tissues: normal (top panel) and tumor (bottom panel). Left: Hematoxylin & Eosin (H&E) staining of tissue sections ( $100\times$ ). Middle: Representative pictures of tissue sections before, during, and after LCM. Right: Targeted cells captured on the cap. Scale bar =  $100 \mu\text{m}$ . (B) Quantitative real-time PCR analysis of GLUT2 expression in human normal and hepatocel-

lular carcinoma cells captured by LCM. Three samples were analyzed in each group, and values are the mean  $\pm$  SEM.  $*P < 0.05$ . (C) Immunohistochemical analysis of GLUT2 protein levels in human hepatocellular carcinoma tissues. The arrowhead indicates representative GLUT2 immunoreactive cells (green). Scale bar =  $20 \mu\text{m}$ . (D) Quantitative real-time PCR analysis of GLUT2 expression in human normal and cancer cell lines. Three samples were analyzed in each group, and values are mean  $\pm$  SEM.

hepatocytes (Figure 1B). Immunohistochemical analysis was performed, and the intensity of GLUT2 positive-cells was compared between normal and hepatoma tissues. Staining for GLUT2 protein was intense in the cytosol of hepatoma cells (Figure 1C, lower panel, arrowhead). Real-time PCR analysis was also used to measure GLUT2 mRNA expression in human hepatoma (Hep G2, Hep 3B), colon cancer (HT 29, COLO 205), and leukemia (HL 60), as well as in normal colon epithelial (FHC) cells as a control. As shown in Figure 1D, more than 200–1000 copies of

the GLUT2 transcript per  $\mu\text{g}$  of mRNA were detected in the Hep G2 and Hep 3B cell lines. In contrast, a lower copy number of GLUT2 was detected in the other cell lines (Figure 1D, bars 3–6). These results suggest that specific GLUT2 expression is required for the growth of these human liver cancer cells.

#### Preferential Cytotoxicity of Ph in Human Cancer Cells

The chemical structure of Ph, a well-known GLUT2-specific inhibitor, is shown in Figure 2A. To ascertain whether GLUT2 is essential for Ph-induced

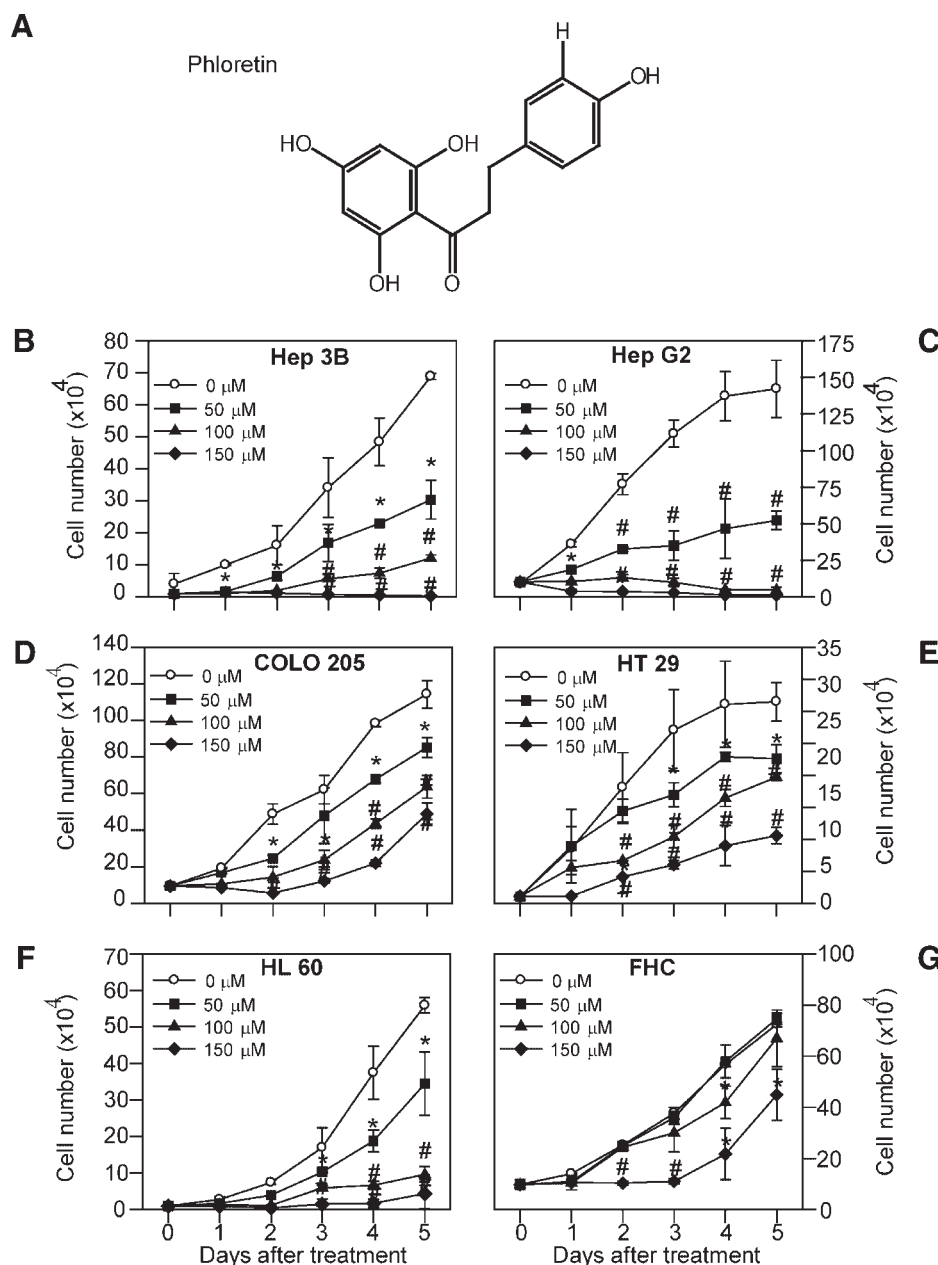


Figure 2. Dose- and time-dependent effects of Ph-induced cell growth inhibition in human cancer and normal cells. (A) The chemical structure of Ph. (B–G) Human Hep G2, Hep 3B, and normal FHC cells were treated with 50–150  $\mu\text{M}$  Ph in a time-dependent manner. Media with or without Ph were renewed daily until the cells were counted. Three samples were analyzed in each group, and values are the mean  $\pm$  SEM. \* $P < 0.05$  and # $P < 0.01$ .

cytotoxicity and therefore whether the two correlate in a cell type-specific manner, Ph cytotoxicity was examined in various cell lines showing different levels of GLUT2 expression: human hepatoma cells (Hep G2 and Hep 3B), which express GLUT2 at extremely high levels; human colon cancer cells (COLO 205 and HT 29), which do not express detectable levels of GLUT2; human leukemia cells (HL 60), which express GLUT2 at low levels; and normal colon epithelial cells (FHC), which do not express detectable levels of GLUT2. These cell lines were treated with Ph and then analyzed for cell growth using a proliferation assay (Figure 2B–G).

Our results show that Ph significantly inhibited the growth of human liver cancer cells (Hep G2 and Hep 3B) when used at a concentration of 50  $\mu\text{M}$  for 1–5 d (Figure 2B and C). However, similar results were also seen in the human cancer cell lines expressing lower levels of GLUT2 (HT 29, COLO 205 and HL60; Figure 2D–F). This implies that GLUT2 was not the only molecular target for Ph-induced cytotoxicity. This cytotoxicity is more likely to be specific to certain cancer cells. To confirm these observations, effects of Ph exposure on normal human colon cells (FHC) and on cancer cells (COLO 205 and HT 29) not expressing GLUT2 were compared. The results show that the FHC cells were very resistant to Ph-induced

cytotoxicity over a concentration range of 50–100  $\mu\text{M}$  (Figure 2G). This suggests that Ph-induced cytotoxicity is cancer cell-specific and acts through cell-specific mechanisms in addition to GLUT2 inhibition.

#### Ph Enhances PTX-Induced Apoptosis in Human Liver Cancer Cells

Next we demonstrated significant apoptosis of Hep G2 cells treated with Ph at concentrations higher than 150  $\mu\text{M}$  for 24 h, based on the results of DNA fragmentation assays (Figure 3A). Recent studies have suggested that drug-induced apoptosis of human malignant cancer cells may be enhanced using a combined treatment protocol that includes anticancer therapeutics with different mechanisms of action. Thus, the present study exposed Hep G2 cells to both Ph and PTX, which induce cell apoptosis and G2/M phase arrest, respectively. After treatment, the cells were examined for the presence of DNA laddering using gel electrophoresis (Figure 3B). DNA laddering was not detected in Hep G2 cells exposed to a low dose of either Ph (50–100  $\mu\text{M}$ ) or PTX (10 nM) for 24 h (Figure 3B, lanes 2–4). Significant DNA fragmentation, however, was observed for Hep G2 cells treated with both agents at the same time

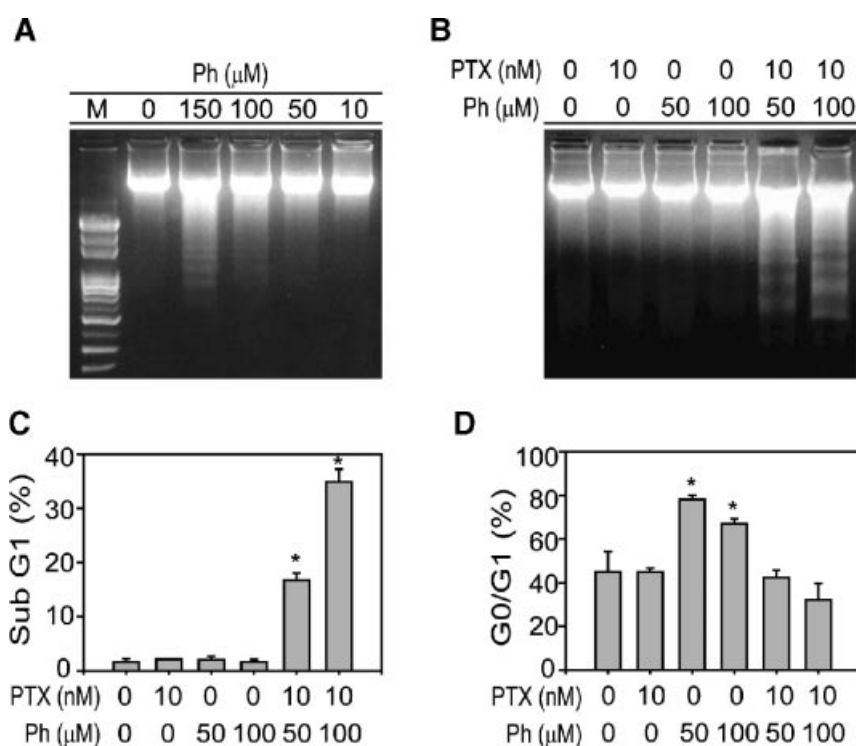


**Figure 3.** Combined treatment with Ph and PTX induces apoptosis in Hep G2 cells. (A) Hep G2 cells were treated with different doses of Ph (10–150  $\mu\text{M}$ ) for 24 h. Induction of apoptosis in Hep G2 cells was demonstrated by DNA fragmentation detected by electrophoresis of genomic DNA. (B) Hep G2 cells were treated with different doses of Ph (50–100  $\mu\text{M}$ ), PTX (10 nM), or both agents. DNA fragmentation was assessed 24 h later. Cells in lane 1 were mock-treated with

DMSO and served as controls. (C–D) Hep G2 cells were treated with Ph (50–100  $\mu\text{M}$ ), PTX (10 nM), or both agents for 24 h. The cells were harvested for flow cytometry analysis. The percentages of cells in the (C) sub-G1 and (D) G0/G1 phases of the cell cycle were determined using the CellFIT DNA analysis software. Three samples were analyzed in each group, and the values are the mean  $\pm$  SEM. \* $P < 0.05$ .

(Figure 3B, lanes 5–6). This finding indicates that Ph enhances PTX-induced apoptosis in Hep G2 cells.

To calculate apoptotic cell death, drug-treated Hep G2 cells were harvested for flow cytometry analysis (Figure 3C). A significant sub-G1 peak was detected for Hep G2 cells following combined treatment with Ph and PTX for 24 h (Figure 3C, bars 5 and 6). Interestingly, significant G0/G1 arrest was induced in Hep G2 cells treated with 50–100  $\mu\text{M}$  Ph for 24 h (Figure 3D, bars 3 and 4). The apoptosis-inducing effects that resulted from combined treatment with Ph and PTX were assessed over time using flow cytometry (Figure 4). These results demonstrate that neither 50  $\mu\text{M}$  Ph nor 10 nM PTX on its own can induce significant apoptosis of Hep G2 cells, even at

48 h posttreatment (Figure 4B and C). Significant apoptosis was induced only in Hep G2 cells exposed to Ph doses greater than 150  $\mu\text{M}$  for more than 24 h (Figure 4D, bar 3). Ph-mediated potentiation of PTX-induced apoptosis was detected in Hep G2 cells (Figure 4E and F).

#### Ph Potentiation of PTX-Induced Apoptosis in Human Liver Cancer Cells Involves Caspase Activation

To further explore the molecular mechanisms of drug-induced apoptosis in Hep G2 cells, the apoptotic mediators, including initiator caspases (8 and 9) and effector caspases (3) caspases, were examined by Western blotting and caspase activity assays (Figure 5A and B). Hep G2 cells were treated either

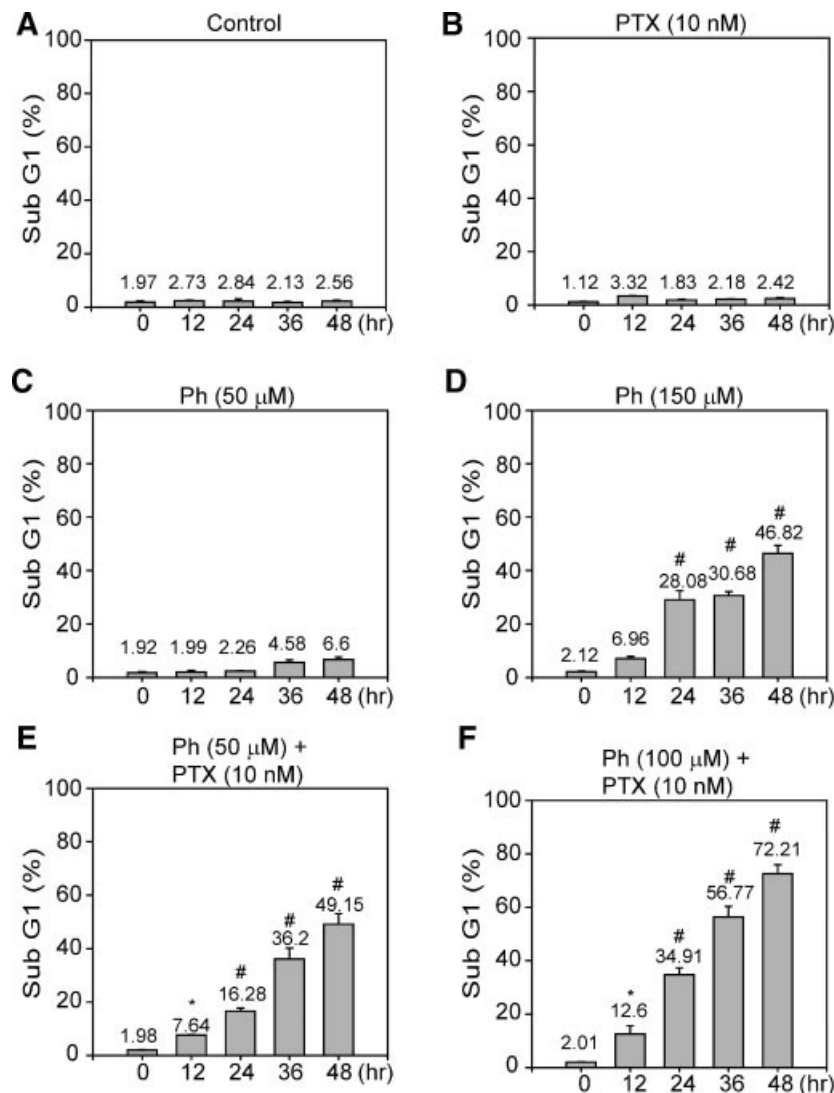


Figure 4. Ph enhances PTX-induced apoptosis of human Hep G2 cells. Human Hep G2 cells were treated with (A) DMSO, (B) PTX (10 nM), (C) Ph (50  $\mu\text{M}$ ), or (D) Ph (150  $\mu\text{M}$ ) for the indicated times. Hep G2 cells were also treated with PTX (10 nM) in combination with (E) Ph (50  $\mu\text{M}$ ) or (F) Ph (100  $\mu\text{M}$ ) for different periods of time. The apoptotic, sub-G1 population of the drug-treated cells was determined by flow cytometry. Three samples were analyzed in each group, and values are the mean  $\pm$  SEM. \* $P < 0.05$  and # $P < 0.01$ .



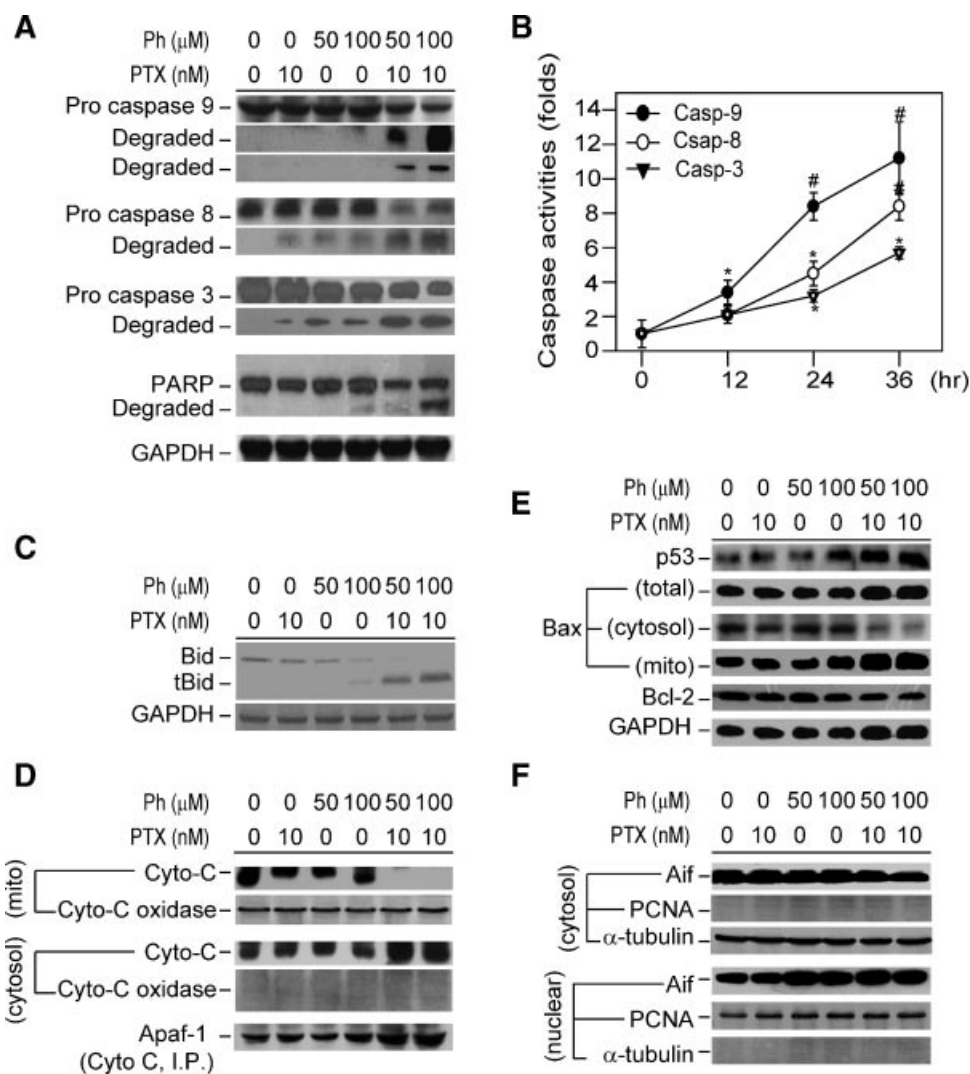


Figure 5. Changes in regulatory protein expression following the Ph potentiation of PTX-induced apoptosis in human Hep G2 cells. (A) Hep G2 cells were treated with DMSO (vehicle), PTX (10 nM), Ph (50–100 μM), or both agents for 24 h. The cells were harvested, and caspase-associated protein expression was determined by Western blot analysis. (B) Hep G2 cells were treated with both Ph (100 μM) and PTX (10 nM) for the indicated time points. After drug treatment,

the cells were harvested and the lysates were used in activity assays for caspases 3, 8, and 9. Three samples were analyzed for each group, and values are the mean ± SEM. \**P* < 0.05 and #*P* < 0.01. (C–F) Hep G2 cells were treated with DMSO, PTX (10 nM), Ph (50–100 μM), or both agents for 24 h. The cells were harvested, and the expression levels of apoptosis-regulatory proteins were determined by Western blot analysis.

with PTX (10 nM), Ph (50–100 μM), or both drugs for 24 h. The results indicate that substantial changes in caspase protein activation were not observed in cells treated with Ph or PTX by themselves (Figure 5A, lanes 2–4). In contrast, combined treatment with both drugs activated caspase 3, as determined by detection of the degraded form of the enzyme, and this activation coincided with the degradation of poly-ADP-ribose polymerase (PARP), a substrate of caspase 3 (Figure 5A, lanes 5 and 6). To further elucidate the apoptotic pathways involved in the activation of caspase 3, we examined changes in caspases 8 and 9 in drug-treated Hep G2 cells. Combined treatment of Hep G2 cells with Ph and PTX activated caspases 8 and 9, as evidenced by

degradation of the procaspases (Figure 5A, lanes 5 and 6). The activities of caspases 3, 8, and 9 were elevated by 3.2-, 4.3-, and 8.6-fold, respectively, in Hep G2 cells treated with both 100 μM Ph and 10 nM PTX for 24 h compared to DMSO-treated control cells (Figure 5B). These observations indicate that caspase activation is involved in drug-induced apoptosis of human liver cancer cells.

#### Ph Potentiation of PTX-Induced Apoptosis Occurs Through Mitochondrial Signaling Pathways That Involve Caspases 8 and 9

Furthermore, we detected the truncated form of Bid (t-Bid) (Figure 5C). This result reveals that the caspase 8 signaling pathway is activated in drug-



treated cells. Our results also demonstrate that combined treatment with Ph and PTX induced a significant increase in the level of cytosolic cytochrome *c* in Hep G2 cells (Figure 5D, lanes 5 and 6). To examine whether the drug-induced release of cytochrome *c* is involved in apoptosome assembly, cytochrome *c* was immunoprecipitated from cytosolic preparations of drug-treated cells. As shown in Figure 5D, Apaf-1 was found to co-immunoprecipitate with cytochrome *c* from Hep G2 cells.

To our knowledge, the p53 protein in Hep G2 cells is wild-type [21,24]. Genes regulated by p53, such as Bax and Bcl-2, play important roles in cellular apoptosis. In the cells treated with both drugs, p53 was significantly induced (Figure 5E). We also found that cytosolic Bax had apparently translocated to the mitochondria, whereas the total level of Bcl-2 protein decreased (Figure 5E, lanes 5 and 6). Translocation of Aif from the cytosol to the nucleus has been shown to activate apoptosis. Our findings demonstrate that combined treatment with both Ph and PTX induces Aif translocation from the mitochondria to the nucleus (Figure 5F). All of these

results support the hypothesis that Ph-mediated apoptosis occurs through mitochondrial signaling pathways, which involve caspases 8 and 9.

#### Ph Potentiation of PTX-Induced Antitumor Effects In Vivo in Hep G2-Xenografted SCID Mice

Next, we examined the therapeutic efficacy of Ph in vivo by administering it to SCID mice bearing Hep G2-xenografted tumors (Figure 6). After the establishment of palpable tumors, with a mean tumor volume of 200 mm<sup>3</sup>, animals received intraperitoneal injections of Ph (10 mg/kg body weight), PTX (1 mg/kg body weight), or both drugs three times per week. Control mice received DMSO in peanut oil vehicle. After 6 wk, the tumor volumes in mice treated with Ph and PTX were significantly smaller than those in animals treated with either Ph or PTX alone (Figure 6A). A reduction in tumor weight of more than fivefold was observed in mice treated with both Ph and PTX compared to those given a vehicle control (DMSO) (Figure 6B). Visible inspection of general appearance and microscopic examination of individual organs showed no gross signs of toxicity,

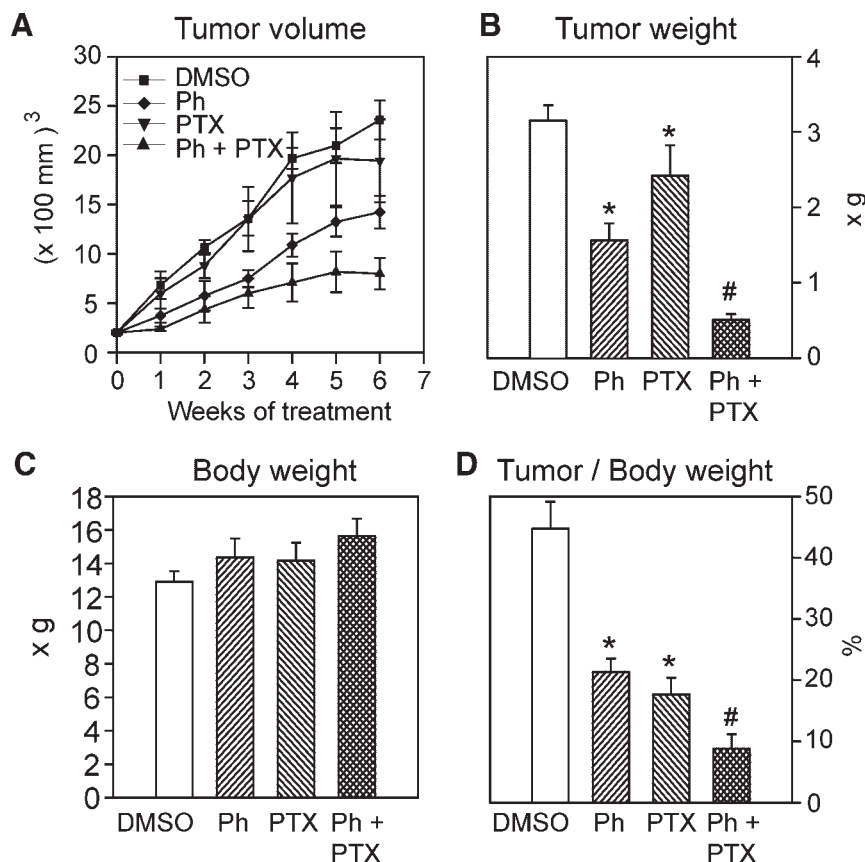


Figure 6. Ph potentiates the antitumor activity of PTX in a human Hep G2-xenografted tumor bearing SCID mouse. (A) Average tumor growth volume of DMSO- versus drug-treated SCID mice ( $n=10$ ). The (B) tumor weight, (C) animal body weight, and (D) tumor/body weight ratio were measured at the end of the experiment. Ten samples were analyzed for each group, and values are the mean  $\pm$  SEM. Comparisons were subjected to ANOVA followed by Fisher's least significant difference test. Significance was accepted at  $P < 0.05$ . \*Groups treated with Ph, PTX, or both differed significantly from the DMSO-treated group. #The combined drug-treated group was significantly different from the groups that received Ph or PTX alone.

including loss of body weight, in any of the mice (Figure 6C and D). These results provide evidence indicating that the Ph potentiation of apoptosis induced by anticancer drugs may aid in the development of novel cancer chemotherapies.

### DISCUSSION

Ph, a natural polyphenolic compound found in apples and pears, has been reported to be a hepatoprotective agent, with studies showing that it prevents tacrine-induced cytotoxicity in human liver cancer cells with an  $EC_{50}$  value of  $37.55 \mu\text{M}$  [37]. Furthermore, Ph at concentrations of  $0.4\text{--}200 \mu\text{M}$  was found to significantly reduce cytotoxicity induced by *tert*-butyl hydroperoxide-induced in rat primary hepatocytes, based on measurements of cellular leakage of lactate dehydrogenase and the serum level of aspartate transaminase [37]. Incubating isolated rat hepatocytes with higher Ph concentrations caused a concentration-dependent decrease in cell viability. The concentration of Ph required to cause a 50% decrease in hepatocyte cell viability ( $LD_{50}$ ) in 2 h was  $>500 \pm 50 \mu\text{M}$  [38]. These results are consistent with several other studies demonstrating that the cell viability of normal rat hepatocytes from *in vivo* perfused rat liver was unaffected by the infusion of Ph at  $200 \mu\text{mol/L}$  [39,40]. The results of this literature suggest that it may be possible to use the apple polyphenolic compound Ph for chemoprevention to reduce the growth of liver cancer cells and induce their apoptosis [41].

Combination therapy is considered to be more effective than monotherapy for prolonging life. A combination regime also reduces side effects because the doses of the drugs used in the treatment are lower than in monotherapy. For example, the starting PTX dose recommended for combined therapy with other antineoplastic drugs, which is as low as  $70 \text{ mg/m}^2$ , is only two-thirds of the dose recommended for PTX monotherapy [42]. A toxicokinetic study demonstrated that the level of PTX in the blood of patients given  $70 \text{ mg/m}^2$  PTX for 24 h was  $17\text{--}27 \text{ ng/mL}$  (corresponding to  $19.9\text{--}31.6 \mu\text{M}$ ) [42]. These results imply that administering PTX at a concentration that results in a serum PTX level below  $19.9 \mu\text{M}$  may decrease toxic side effects. In this study, we demonstrate that  $10 \text{ nM}$  PTX does not induce Hep G2 apoptosis (Figure 4B, sub-G1 population = 2.42%). However, when  $10 \text{ nM}$  PTX was used in combination with  $50 \mu\text{M}$  Ph, apoptosis in Hep G2 cells jumped from 2.42% to 49.15%. *In vivo* experiments show that combined therapy reduced tumor weight by more than fourfold compared to treatment with PTX alone. These results are consistent with the *in vitro* study results and confirm the antitumor effects of combination regimens.

Ph at concentrations up to  $100 \mu\text{M}$  has been reported to inhibit the growth of several cancer cells and to induce apoptosis of HT 29, B16 melanoma,

and HL 60 human leukemia cells [9,43,44]. Our results confirm that the Ph-induced cytotoxic effect is cancer cell-specific and occurs via mechanisms in addition to GLUT2 inhibition. PKC is involved in carcinogenesis, proliferation, apoptosis, and metastasis of liver cancer [45]. New anticancer strategies have been developed with PKC as a potential target for therapeutic intervention. However, most of the encouraging preliminary data have been observed only in liver cancer cell lines [46]. New possibilities for anticancer treatment came with the report that the apple polyphenolic compound Ph significantly inhibits different types of cytosolic PKC isoforms in human colon cancer cells (HT 29) [47]. Ph-induced apoptosis was also demonstrated in human HL 60 and multiple myeloma cells [9,48,49]. Similar results were reported by another group, who found that the inhibition of PKC activity increases the susceptibility of HT-29 cells to PTX-induced apoptosis, and that phorbol ester induction of PKC reduces this susceptibility [50]. All of these reports suggest that deregulation of the PKC signaling plays a role in tumor progression. Therefore, PKC has been exploited as a target for antitumor treatment [51]. Additional studies should be performed to investigate whether Ph exerts antitumor effects on liver cancer cells by inhibiting PKC.

At least in some tumors, PKC inhibition appears to be essential for reducing growth or inducing apoptosis. It has been difficult to gain deeper insight into this observation, since none of the PKC inhibitors currently available is specific to individual PKC isoenzymes. Despite these problems, PKC modulators such as miltefosine, bryostatin, safingol, CGP41251, and UCN-01 are currently being used in the clinic or are in clinical trials. The important question is whether PKC is the molecular target of Ph, since this drug also is known to interfere with other molecular targets, such as GLUT2. Our results fail to resolve this question; in fact, they are consistent with the possibility that Ph induces apoptosis by inhibiting both GLUT2 or PKC inhibition, depending on the cell type or culture conditions. Our results suggest that Ph in human cancer cells participates not only in these PKC-mediated signaling pathways but also in pathways that are linked to the PKC ones. For example, Ph-induced apoptosis depends on many additional factors, including p53, bcl-2, and bax (Figure 5). Furthermore, our results provide detail into the molecular mechanism of Ph-mediated caspase activation, since mitochondria in liver cancer cells were found to signal the stimulation that eventually triggered apoptosis. Consistent with our results, another study detected that caspase activation, DNA fragmentation, and cleavage of poly(ADP ribose) polymerase in Ph-induced colon cancer cells (HT 29) [43].

These studies point up the contradictory results that have been reported concerning the ability of Ph

to inhibit PKC expression and modulate apoptosis in human cancer cells. Nevertheless, this study clearly shows that combining antitumor drugs (such as PTX) with PKC modulators (such as Ph) can enhance the effects of the former. A major challenge for future research is to determine whether PKC modulation can be used to improve cancer therapy.

#### ACKNOWLEDGMENTS

This study was supported by grants from the National Science Council of ROC (NSC 95-2320-B-038-011 to Dr. Ho, and NSC 95-2314-B-038-006 to Dr. Wu), and by funding from the Shin Kong Wu Ho-Su Memorial Hospital (SKH-TMU-94-06).

#### REFERENCES

- Godoy A, Ulloa V, Rodriguez F, et al. Differential subcellular distribution of glucose transporters GLUT 1-6 and GLUT9 in human cancer: Ultrastructural localization of GLUT1 and GLUT5 in breast tumor tissues. *J Cell Physiol* 2006;207:614–627.
- Garcia MA, Millan C, Balmaceda-Aguilera C, et al. Hypothalamic ependymal-glia cells express the glucose transporter GLUT2, a protein involved in glucose sensing. *J Neurochem* 2003;86:709–724.
- Fukumoto H, Seino S, Imura H, et al. Sequence, tissue distribution, and chromosomal localization of mRNA encoding a human glucose transporter-like protein. *Proc Natl Acad Sci USA* 1988;85:5434–5438.
- Yamamoto T, Seino Y, Fukumoto H, et al. Over-expression of facilitative glucose transporter genes in human cancer. *Biochem Biophys Res Commun* 1990;170:223–230.
- Brown RS, Wahl RL. Overexpression of Glut-1 glucose transporter in human breast cancer. An immunohistochemical study. *Cancer* 1993;72:2979–2985.
- Noguchi Y, Marat D, Saito A, et al. Expression of facilitative glucose transporters in gastric tumors. *Hepato-gastroenterology* 1999;46:2683–2689.
- Lee JD, Yang WI, Park YN, et al. Different glucose uptake and glycolytic mechanisms between hepatocellular carcinoma and intrahepatic mass-forming cholangiocarcinoma with increased (18)F-FDG uptake. *J Nucl Med* 2005;46:1753–1759.
- Younes M, Lechago LV, Somoano JR, Mosharaf M, Lechago J. Wide expression of the human erythrocyte glucose transporter Glut1 in human cancers. *Cancer Res* 1996;56:1164–1167.
- Kern M, Pahlke G, Balavenkatraman KK, Bohmer FD, Marko D. Apple polyphenols affect protein kinase C activity and the onset of apoptosis in human colon carcinoma cells. *J Agric Food Chem* 2007.
- Jordan NJ, Holman GD. Photolabelling of the liver-type glucose-transporter isoform GLUT2 with an azitrifluoroethylbenzoyl-substituted bis-D-mannose. *Biochem J* 1992;286:649–656.
- Walker J, Jijon HB, Diaz H, Salehi P, Churchill T, Madsen KL. 5-aminoimidazole-4-carboxamide riboside (AICAR) enhances GLUT2-dependent jejunal glucose transport: A possible role for AMPK. *Biochem J* 2005;385:485–491.
- Lin YP, Hsu FL, Chen CS, Chern JW, Lee MH. Constituents from the Formosan apple reduce tyrosinase activity in human epidermal melanocytes. *Phytochemistry* 2007;68:1189–1199.
- Sands JM, Timmer RT, Gunn RB. Urea transporters in kidney and erythrocytes. *Am J Physiol* 1997;273:F321–F339.
- Tombola F, Morbiato L, Del Giudice G, Rappuoli R, Zoratti M, Papini E. The *Helicobacter pylori* VacA toxin is a urea permease that promotes urea diffusion across epithelia. *J Clin Invest* 2001;108:929–937.
- Hertel C, Terzi E, Hauser N, Jakob-Rotne R, Seelig J, Kemp JA. Inhibition of the electrostatic interaction between beta-amyloid peptide and membranes prevents beta-amyloid-induced toxicity. *Proc Natl Acad Sci USA* 1997;94:9412–9416.
- Wani MC, Taylor HL, Wall ME, Coggon P, McPhail AT. Plant antitumor agents. VI. The isolation and structure of taxol, a novel antileukemic and antitumor agent from *Taxus brevifolia*. *J Am Chem Soc* 1971;93:2325–2327.
- Ho YS, Duh JS, Jeng JH, et al. Griseofulvin potentiates antitumorigenesis effects of nocodazole through induction of apoptosis and G2/M cell cycle arrest in human colorectal cancer cells. *Int J Cancer* 2001;91:393–401.
- Azzoli CG, Krug LM, Gomez J, et al. A phase 1 study of pralatrexate in combination with paclitaxel or docetaxel in patients with advanced solid tumors. *Clin Cancer Res* 2007;13:2692–2698.
- Camacho LH, Kurzrock R, Cheung A, et al. Pilot study of regional, hepatic intra-arterial paclitaxel in patients with breast carcinoma metastatic to the liver. *Cancer* 2007;109:2190–2196.
- Brenes O, Arce F, Gatzjens-Boniche O, Diaz C. Characterization of cell death events induced by anti-neoplastic drugs cisplatin, paclitaxel and 5-fluorouracil in human hepatoma cell lines: Possible mechanisms of cell resistance. *Biomed Pharmacother* 2007;61:347–355.
- Lee WS, Chen RJ, Wang YJ, et al. In vitro and in vivo studies of the anticancer action of terbinafine in human cancer cell lines: G0/G1 p53-associated cell cycle arrest. *Int J Cancer* 2003;106:125–137.
- Niewolik D, Wojtesek B, Kovarik J. p53 derived from human tumour cell lines and containing distinct point mutations can be activated to bind its consensus target sequence. *Oncogene* 1995;10:881–890.
- Ho YS, Wang YJ, Lin JK. Induction of p53 and p21/WAF1/CIP1 expression by nitric oxide and their association with apoptosis in human cancer cells. *Mol Carcinog* 1996;16:20–31.
- Bressan B, Galvin KM, Liang TJ, Isselbacher KJ, Wands JR, Ozturk M. Abnormal structure and expression of p53 gene in human hepatocellular carcinoma. *Proc Natl Acad Sci USA* 1990;87:1973–1977.
- Siddiqui KM, Chopra DP. Primary and long term epithelial cell cultures from human fetal normal colonic mucosa. *In Vitro* 1984;20:859–868.
- Ho YS, Wu CH, Chou HM, et al. Molecular mechanisms of econazole-induced toxicity on human colon cancer cells: G0/G1 cell cycle arrest and caspase 8-independent apoptotic signaling pathways. *Food Chem Toxicol* 2005;43:1483–1495.
- Wu CH, Jeng JH, Wang YJ, et al. Antitumor effects of miconazole on human colon carcinoma xenografts in nude mice through induction of apoptosis and G0/G1 cell cycle arrest. *Toxicol Appl Pharmacol* 2002;180:22–35.
- Singh SV, Herman-Antosiewicz A, Singh AV, et al. Sulforaphane-induced G2/M phase cell cycle arrest involves checkpoint kinase 2-mediated phosphorylation of cell division cycle 25C. *J Biol Chem* 2004;279:25813–25822.
- Ho YS, Ma HY, Chang HY, et al. Lipid peroxidation and cell death mechanisms in rats and human cells induced by chloral hydrate. *Food Chem Toxicol* 2003;41:621–629.
- Lin SY, Chang YT, Liu JD, et al. Molecular mechanisms of apoptosis induced by magnolol in colon and liver cancer cells. *Mol Carcinog* 2001;32:73–83.
- Abe N, Watanabe T, Ozawa S, et al. Pancreatic endocrine function and glucose transporter (GLUT)-2 expression in rat acute pancreatitis. *Pancreas* 2002;25:149–153.
- Johnson JH, Ogawa A, Chen L, et al. Underexpression of beta cell high Km glucose transporters in noninsulin-dependent diabetes. *Science* 1990;250:546–549.

33. Aerts JL, Gonzales MI, Topalian SL. Selection of appropriate control genes to assess expression of tumor antigens using real-time RT-PCR. *BioTechniques* 2004;36:84–86 88, 90-81.
34. Huang C, Yang L, Li Z, et al. Detection of CCND1 amplification using laser capture microdissection coupled with real-time polymerase chain reaction in human esophageal squamous cell carcinoma. *Cancer Genet Cytogenet* 2007; 175:19–25.
35. Doi C, Noguchi Y, Ito T, Yoshikawa T, Makino T, Matsumoto A. Alteration in immunoeexpression of glucose transporter 2 in liver of tumour-bearing rats. *Int J Exp Pathol* 1998;79:25–31.
36. Ogawa A, Kurita K, Ikezawa Y, et al. Functional localization of glucose transporter 2 in rat liver. *J Histochem Cytochem* 1996;44:1231–1236.
37. An RB, Park EJ, Jeong GS, Sohn DH, Kim YC. Cytoprotective constituent of *Hovenia Lignum* on both Hep G2 cells and rat primary hepatocytes. *Arch Pharm Res* 2007;30:674–677.
38. Moridani MY, Galati G, O'Brien PJ. Comparative quantitative structure toxicity relationships for flavonoids evaluated in isolated rat hepatocytes and HeLa tumor cells. *Chem Biol Interact* 2002;139:251–264.
39. vom Dahl S, Haussinger D. Evidence for a phloretin-sensitive glycerol transport mechanism in the perfused rat liver. *Am J Physiol* 1997;272:G563–G574.
40. vom Dahl S, Haussinger D. Characterization of phloretin-sensitive urea export from the perfused rat liver. *Biol Chem Hoppe Seyler* 1996;377:25–37.
41. Kim ES, Hong WK. An apple a day does it really keep the doctor away? The current state of cancer chemoprevention. *J Natl Cancer Inst* 2005;97:468–470.
42. Yonemoto H, Ogino S, Nakashima MN, Wada M, Nakashima K. Determination of paclitaxel in human and rat blood samples after administration of low dose paclitaxel by HPLC-UV detection. *Biomed Chromatogr* 2007;21:310–317.
43. Park SY, Kim EJ, Shin HK, et al. Induction of apoptosis in HT-29 colon cancer cells by phloretin. *J Med Food* 2007;10:581–586.
44. Kobori M, Iwashita K, Shinmoto H, Tsushida T. Phloretin-induced apoptosis in B16 melanoma 4A5 cells and HL60 human leukemia cells. *Biosci Biotechnol Biochem* 1999;63: 719–725.
45. Wu TT, Hsieh YH, Wu CC, Hsieh YS, Huang CY, Liu JY. Overexpression of protein kinase C alpha mRNA in human hepatocellular carcinoma: A potential marker of disease prognosis. *Clin Chim Acta* 2007;382:54–58.
46. Zhu BH, Yao ZX, Luo SJ, et al. Effects of antisense oligonucleotides of PKC-alpha on proliferation and apoptosis of HepG2 in vitro. *Hepatobiliary Pancreat Dis Int* 2005;4: 75–79.
47. Kern M, Pahlke G, Balavenkatraman KK, Bohmer FD, Marko D. Apple polyphenols affect protein kinase C activity and the onset of apoptosis in human colon carcinoma cells. *J Agric Food Chem* 2007;55:4999–5006.
48. Savickiene J, Gineitis A, Stigbrand T. Modulation of apoptosis of proliferating and differentiating HL-60 cells by protein kinase inhibitors: Suppression of PKC or PKA differently affects cell differentiation and apoptosis. *Cell Death Differ* 1999;6:698–709.
49. Neri A, Marmioli S, Tassone P, et al. The oral PKC-beta inhibitor enzastaurin (LY317615) suppresses signalling through the AKT pathway, inhibits proliferation and induces apoptosis in multiple myeloma cell lines. *Leuk Lymphoma* 2008;1–10.
50. Cesaro P, Raiteri E, Demoz M, et al. Expression of protein kinase C beta1 confers resistance to TNFalpha- and paclitaxel-induced apoptosis in HT-29 colon carcinoma cells. *Int J Cancer* 2001;93:179–184.
51. Hofmann J. Modulation of protein kinase C in antitumor treatment. *Rev Physiol Biochem Pharmacol* 2001;142:1–96.